

CERN-TH-2000-223
DAMTP-2000-72

PHYSICS AT HIGH Q^2 AND p_t^2 : SUMMARY OF DIS 2000

M. KUZE

Institute of Particle and Nuclear Studies, KEK, Tsukuba 305-0801, Japan

S. LOLA

CERN Theory Division, CH-1211, Geneva 23, Switzerland

E. PEREZ

CEA Saclay, DSM/DAPNIA/Spp, 91191 Gif-sur-Yvette, France

B. ALLANACH

DAMTP, Wilberforce Rd, Cambridge CB3 0WA, UK

We summarize the experimental and theoretical results presented in the “Physics at the Highest Q^2 and p_t^2 ” working group at the DIS 2000 Workshop. High Q^2 and p_t^2 processes measured at current and future colliders allow to improve our knowledge of Standard Model (SM) physics, by providing precise measurements of the SM parameters and, consequently, consistency checks of the SM. Moreover, they give information on key quantities for the calculation of the SM expectations in a yet unexplored domain, such as the parton densities of the proton or the photon. In addition to these experimental inputs, higher-order calculations are also needed to obtain precise expectations for SM processes, which are a key ingredient for the searches for new phenomena in high Q^2 and p_t^2 processes at current and future experiments. The experimental and theoretical status of SM physics at high Q^2 and p_t^2 is reviewed in the first part of this summary, with the remaining being dedicated to physics beyond the Standard Model.

1 Jet Physics at High p_t^2 and Q^2

The production of jets at high-energy colliders is a very good testing ground of perturbative QCD, and a tool for determining the parton distribution functions of the proton and the photon. Possible deviation from the QCD predictions at the highest energy scales would be a hint for unrevealed new physics. A good understanding of exclusive multi-jet final states is also crucial in many searches for new-particle productions, such as the production and decay of R -parity-violating squarks.

The status of jet production at HERA was reviewed in the photoproduction¹ and DIS² regions. In photoproduction, dijet cross-sections have been measured up to $p_{t,jet} \approx 80$ GeV and $m_{jj} \approx 150$ GeV, and three-jet cross-sections up to $m_{jjj} \approx 200$ GeV. In the direct-photon regime the measurements are in good agreement with the NLO QCD predictions, while in the resolved-photon regime one finds a discrepancy, which could be attributed to the limited knowledge of the photon structure functions.

In the DIS region, dijet cross-sections can be used to extract the strong coupling constant α_s . Also, dijet production at very high Q^2 , $Q^2 \approx 10^4 \text{ GeV}^2$, has been studied in both neutral current (NC) and charged current (CC) processes (Fig. 1). Even at these extremely short distances, the NLO QCD predictions work very well within the statistics of the current data.

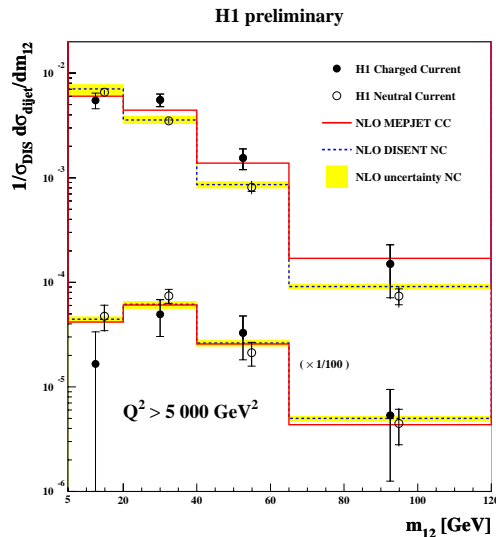


Figure 1: Dijet mass distribution for NC/CC DIS at very high Q^2 , compared to NLO QCD predictions.

At TeVatron³, thanks to the large center-of-mass energy, the inclusive jet production has been measured up to $p_{t,jet} \approx 500 \text{ GeV}$. Moreover, the angular distribution has been studied. The data indicate better agreement with predictions using proton structure functions in which the gluon distribution has been increased at large x .

At the near-future programs TeVatron Run II and HERA lumi-upgrade, more precise tests at highest p_t^2 and Q^2 will provide a better knowledge of structure functions, which is a crucial element for future searches at the LHC. In some measurements, the dominant errors arise due to the lack of accuracy of the theoretical predictions. State-of-the-art calculations from the theorists' point of view have been presented⁴. A number of NLO programs are available, and theorists are working hard for the next step, i.e. NNLO programs. Generally, calculation programs for $\bar{p}p$ and e^+e^- are more advanced than ep in terms of parton multiplicity. Also, only one NLO program for ep can include electroweak couplings. With high-statistics measurements anticipated, the HERA experimentalists strongly wish for developments in this field.

2 Electroweak Physics and high Q^2 DIS

The latest results on electroweak measurements from LEP2⁵ and TeVatron⁶ have been reviewed. The W -pair production cross-section at LEP2 has been presented up to a center-of-mass energy of 202 GeV, and the data agree very well with recent detailed theoretical calculations such as **RacoonWW**. The latest LEP2-combined W -mass measurement gives $M_W = 80.401 \pm 0.048$ GeV. The Higgs search has so far yielded no signal, leading to $m_H > 107.7$ GeV. At TeVatron, a combined measurement of the W -mass yields $M_W = 80.448 \pm 0.062$ GeV. The W -width is also measured. The Run II prospects were presented, including an expected top-mass measurement with a 3 GeV accuracy (currently about 5 GeV) and a W -mass precision of 40 MeV per experiment.

The latest results on high- Q^2 cross-section measurements in NC and CC DIS processes at HERA were reviewed by H1⁷ and ZEUS⁸. Both e^+p and e^-p datasets are available. In the NC data, the e^-/e^+ cross-sections start to separate at large Q^2 , where Z -exchanges give a significant contribution. The difference is essentially xF_3 , which is proportional to the difference between the quark and antiquark densities in leading order. ZEUS has extracted xF_3 for $Q^2 > 3000$ GeV² for the first time (Fig. 2). Although the statistical accuracy is limited, the result is consistent with the SM prediction with recent parton-density fits. For the CC process, different electron charge means probing different quark flavors. The Q^2 -dependence is driven by the W -propagator mass, giving a space-like measurement of M_W . H1 has presented the double differential cross-section $d^2\sigma/dxdQ^2$ from recent e^-p data, as compared to e^+p . Clearly a higher cross-section for e^-p than e^+p is seen, and the difference increases as Q^2 increases.

Reports have been made on the future electroweak physics at the upgraded HERA, from both the theoretical⁹ and the experimental¹⁰ point of view. Using high-statistics CC and NC data, constraints of about 50 MeV on M_W in the space-like region can be obtained; however, this is true only if the systematic uncertainties can be controlled at the 1–2% level. This is a challenge for experimentalists (e.g. detector energy scale), as well as for theorists (e.g. reduction of the scale uncertainties in the higher-order calculation). Moreover, the error from the parton-density functions has to be substantially reduced.

One of the important features of the HERA upgrade is the introduction of longitudinal electron polarization to collider experiments. It has been shown that high polarization, as well as its accurate measurement, is essential to many studies, e.g. to determine the vector and axial-vector coupling of light quarks.

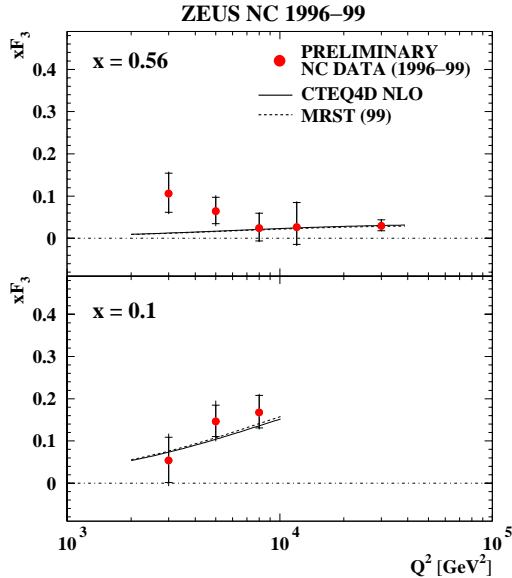


Figure 2: Extracted xF_3 , plotted as a function of Q^2 , at two different x values.

3 W/Z Production, High- p_t leptons

The on-shell production of the W/Z gauge bosons is an interesting test of non-trivial SM calculations which involve gauge cancellations, resummations and higher-order corrections (both QCD and electroweak). The recent status of the theoretical calculations and the understanding of uncertainties has been reviewed¹¹. At LEP2, W -pair production is predicted to an accuracy of about 0.1%, in very good agreement with the measurements. For W production at TeVatron, the electroweak one-loop corrections and the NNLO QCD corrections are available. On the other hand, the calculation for HERA is not as advanced as those mentioned above, although a recent calculation of the QCD correctios for $ep \rightarrow eWX$ process¹² is worth noting. With the upcoming high-statistics productions at the upgraded HERA, more work on this field is desired.

Experimental results on the QCD aspects of W/Z production at TeVatron have been presented¹³. The high-statistics W production allows for an accurate comparison of the $p_t(W)$ distribution with NNLO QCD predictions, and good agreement is observed. In addition, $p_t(Z)$ is compared with the theoretical calculations at both the low- and high- p_t regions. At low p_t , soft

Table 1: Compilation of events with an isolated high- p_t lepton and missing p_t found by H1 and ZEUS. The numbers show the observed/expected events for electron (e), muon (μ) and the sum ($e + \mu$).

H1				ZEUS			
Data period	e	μ	$e + \mu$	Data period	e	μ	$e + \mu$
94-97 e^+p (36.5 pb $^{-1}$)	0/0.50	5/0.56	5/1.06	94-97 e^+p (48 pb $^{-1}$)	3/3.5	0/2.0	3/5.5
98-99 e^-p (12.8 pb $^{-1}$)	0/0.25	0/0.24	0/0.49	98-99 e^-p (16 pb $^{-1}$)	2/0.8	0/0.8	2/1.6
99-00 e^+p (24.9 pb $^{-1}$)	2/0.60	1/0.51	3/1.11	99 e^+p (18 pb $^{-1}$)	2/1.8	4/0.9	6/2.7
Σ (74.2 pb $^{-1}$)	2/1.35	6/1.31	8/2.66	Σ (82 pb $^{-1}$)	7/6.1	4/3.7	11/9.8

gluon radiation dominates, requiring resummation of large logarithmic terms and handling of non-perturbative contributions. The predictions successfully describe the data over the whole p_t range.

Closely related to W production, events with an isolated lepton (e or μ) and missing p_t (attributed to the neutrino) have drawn considerable attention at HERA, mainly due to the muon events observed by the H1 experiment in the 1994-97 e^+p data. The rate of these events, as well as the distribution of the kinematic variables, are largely different from the SM expectations, where the dominant contribution comes from the W production. The ZEUS experiment, on the other hand, observed no such excess and its results were consistent with the SM. An update with 1998-99 e^-p data was done by both collaborations last summer, and no deviation was reported by either experiment.

In this conference, the results from the 1999-2000 e^+p data were presented¹⁴ from both H1 and ZEUS. ZEUS finds two electron events and four muon events from the 1999 data, where 1.8 and 0.9 events are expected, respectively. Although the rate of muon events is higher than expected in this dataset, when combined with the previous datasets in which no muon event was observed, the total sample shows good agreement with the expectations (7 electron events seen with 6.1 ± 0.9 expected, and 4 muon events seen with 3.7 ± 0.4 expected). Moreover, the events show a back-to-back topology between the muon and the hadronic system, typical of a SM $\gamma\gamma \rightarrow \mu\mu$ process in which one of the muons has very low p_t , with the p_t of the hadronic final state, p_T^X , being not too large. The distributions of p_T^X and of the μ -hadrons acoplanarity of the μ events are compared to the SM expectations in Fig. 3, where the μ events observed by H1 in the 1994-97 e^+p data are also indicated as vertical arrows.

From the 1999-2000 data, H1 has observed two electron events and one

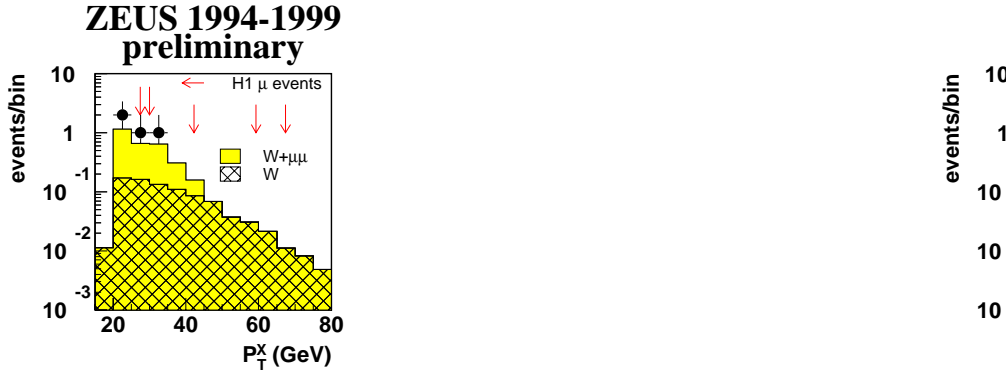


Figure 3: Distributions of the acoplanarity between the muon and the hadronic system (left), and of the p_t of the hadronic final state p_T^X (right) of the four μ events observed by ZEUS in the 1999 data. The histograms show the SM backgrounds expected in the ZEUS analysis for the 1994-99 luminosity. The arrows indicate the acoplanarity and p_T^X of the five μ events observed by H1 in the 1994-97 data.

muon event, all with fairly large hadronic p_t , greater than 40 GeV. Summing the electron and muon events from all datasets, the total number of H1 events in the region of hadronic $p_t > 25$ GeV is 8, with the SM expectation being 2.66 ± 0.60 . The detailed breakdown is shown in Table 1. Note that the expected number of events for H1 is generally smaller than for ZEUS, due to additional cuts to enhance the W events and suppress other SM processes. Combined efforts towards a detailed understanding of the differences have started between the two collaborations.

4 Parton Densities at high x

A precise knowledge of the SM expectations is a key ingredient for the searches for new phenomena described in the remaining part of this report. In general, new physics is already constrained to appear at the highest accessible scales, where (at ep and hadronic colliders) high- x incoming partons are involved. Hence, the precise knowledge of the high- x parton densities in the proton is crucial for new physics searches. It was shown^{15,16} that the parton densities in the high- x region are not so well constrained by the existing data. This is in particular the case for the d -quark density, which is not constrained by the W asymmetries at the TeVatron¹³ for $x > 0.3$. For higher x values, information

on $d(x)$ is obtained from the F_2^d data, but the size of the nuclear corrections which have to be applied is unknown. This large uncertainty on $d(x)$ at high x could be significantly reduced from the future HERA CC e^+p data.

5 Single Top Production

The cross-section for single top production at the TeVatron II is ~ 3.3 pb. Although this is 3 orders of magnitude smaller than the W +jets production rate, it was shown¹⁷ that the extraction of the single top signal is possible. This allows to carry out specific measurements, such as the total top decay width or the Cabibbo-Kobayashi-Maskawa matrix element V_{tb} . Moreover, single top production is a gold-plated process to search for new physics.

At LEP and HERA, the SM production cross-section for single top is tiny. However, higher-order operators may allow a top quark coupling to a light quark and a gauge boson, which would lead to flavor-changing neutral current (FCNC) single top production at LEP2 and HERA. The cross-sections depend on the size of the anomalous couplings κ_V at the tqV vertices ($V = \gamma, Z$), which are constrained by upper limits of the branching ratio $t \rightarrow V + u/c$. Single top production followed by $t \rightarrow Wb$ has been investigated by the LEP experiments¹⁸, exploiting the fact that the b -quark is emitted at a quasi-fixed energy. Some candidate events were observed, but no excess over the SM background (mainly from WW production) was reported; upper limits on the anomalous couplings were derived, improving the TeVatron bounds on κ_Z . However, LEP data provide less sensitivity on κ_γ , and the full coming LEP2 data should only marginally improve the bound set by $BR(t \rightarrow \gamma q)$ on this coupling. It is interesting to note that, for κ_γ equal to its upper bound, the cross-section for single top production at HERA via $eu \rightarrow et$ is ~ 1 pb and could thus be observable. In particular, the leptonic decays of the W would give rise to events with a high- p_t isolated lepton and a very energetic hadronic final state, similar to those discussed in section 3.

6 Excited Fermions

Excited fermions (f^*) would be a clear evidence for fermion substructure. At HERA, these could be singly produced via the t -channel exchange of a gauge boson, and would subsequently decay into a SM fermion and a boson V . Collider searches are generally interpreted in the framework of the phenomenological model¹⁹, where the interactions of f^* with a SM fermion and an electroweak boson (a gluon) are parameterized via the compositeness scale Λ and relative couplings f and f' (f_s).

Final results from a search for e^* , ν^* and q^* using the 94-97 e^+p data have

been reported by the H1 Collaboration at this conference²⁰. The decays of f^* into γ , Z and W , followed by the subsequent decay of the boson into e , μ , ν or hadrons have been investigated, and no deviation from the SM predictions have been observed. This leads to constraints on the considered model, which complement the bounds derived by other experiments. In particular, while the TeVatron sets very stringent bounds²¹ on excited quarks q^* produced in qg fusion via the coupling constant f_s ($M(q^*) > 760$ GeV for $f = f' = f_s$), the limits obtained at HERA are better, provided f_s is smaller than ~ 0.1 , as illustrated in Fig. 4.

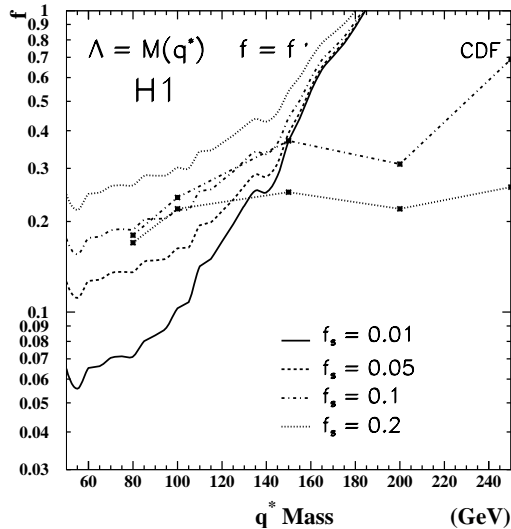


Figure 4: Constraints on q^* assuming $f = f'$ and $\Lambda = M(q^*)$ for different f_s values, as obtained by the H1 and CDF experiments.

In addition, excited neutrinos ν^* have been searched for by both Collaborations in the e^-p data accumulated in 98-99, via their decay $\nu^* \rightarrow \nu\gamma$. The preliminary resulting bound improved significantly the one obtained from the larger statistics e^+p sample, due to the significantly higher production cross-section. Under the assumption $f/\Lambda = 1/M(\nu^*)$, ν^* lighter than 161 GeV can be excluded at 95% confidence level.

7 New $eeqq$ interactions

7.1 Contact Interactions

Contact Interactions (CI) can be used to parameterize any new physics process appearing at an energy scale Λ above the center-of-mass energy \sqrt{s} . At HERA, TeVatron and LEP, $eeqq$ contact interactions would interfere (constructively

or destructively) with SM processes, namely NC DIS, Drell-Yan and $q\bar{q}$ production.

The H1 and ZEUS Collaborations searched for such distortions in the full e^+p data collected between 1994 and 1997²². An update of these results²² was obtained by H1, by including the e^-p data, which allowed to significantly improve the limits on the scale Λ for some models. The resulting bounds depend on the CI model and reach 6.4 TeV, being competitive with or better than the corresponding limits obtained at the TeVatron from high-mass Drell-Yan ee events²¹. In contrast to the more stringent limits obtained by the LEP experiments, these bounds do not rely on the flavor symmetry hypothesis. The CI analysis has been interpreted by the H1 Collaboration in terms of quark radius, applying a multiplicative form factor to the SM $d\sigma/dQ^2$. Very heavy new bosons (leptoquarks) coupling to $e - q$ pairs have also been constrained. In addition, constraints on models with large extra dimensions where gravity could become strong at the electroweak scale have been derived for the first time from eq scattering. The mass scale M_s characterising the effective coupling of the tower of Kaluza-Klein gravitons with SM fermions is constrained to be greater than ~ 700 GeV, which is comparable to limits obtained from the ff ($f \neq e$) production at LEP.

7.2 Leptoquarks

Leptoquarks (LQs) are scalar or vector color-triplet bosons which appear in many extensions of the SM and carry both lepton (L) and baryon (B) numbers. At HERA, LQs with fermion number $F = 3B + L = 0$ ($F = 2$) could be resonantly produced via fusion between the incoming positron (electron) and a valence quark coming from the proton. Hence, the e^+p and e^-p data are complementary, since they allow to probe different LQ types. LQs can decay back to $e + q$ with a branching ratio β , leading to NC DIS-like final states.

ZEUS and H1 searched for LQs in the 94-97 e^+p data and final results have been published²³. The H1 analysis makes use of a mass-dependent lower y_{cut} to maximize the significance of a LQ signal, by exploiting the specific angular distribution of the LQ decay products. A slight excess of high- y events is observed in the H1 data for invariant masses around 200 GeV, mainly due to events previously reported in the 94-96 data. ZEUS performed a general $e - q$ resonance search and also reports a slight (not statistically compelling) excess of events at high mass. However, these events are observed at low- y values, which would not be expected from a LQ signal. Both HERA experiments have performed a preliminary analysis of the e^-p dataset, and no deviation from the SM prediction has been observed²⁴. The e^+p (e^-p) analyses allowed stringent

bounds to be set on $F = 0$ ($F = 2$) LQs. In addition, ZEUS presented a first look at the most recent e^+p data accumulated in 1999. No deviation from SM was yet observed in this small statistics (18 pb^{-1}) sample.

The current status on LQs constraints is presented in Fig. 5, for the example case of a $F = 2$ LQ decaying to eq and νq with $\beta = 0.5$. The results are shown as mass-dependent upper bounds on the coupling λ of the LQ to the eq pair. At the TeVatron, LQs are mainly pair-produced via the strong coupling, which results in λ -independent mass bounds²⁵. It can be seen in Fig. 5 that the three colliders explore the (λ, M_{LQ}) plane in a complementary way and, for an electromagnetic strength of the Yukawa coupling λ (i.e. $\lambda = 0.3$), LQ masses up to 290 GeV can be ruled out. Note that for LQs decaying only into $e + q$, a lower mass bound of 242 GeV can be obtained by combining $D\emptyset$ and CDF data.

Alternatively, for a fixed value of the coupling λ , mass-dependent constraints on β were obtained from the HERA data. The derived bounds extend beyond the domain excluded by the TeVatron, for low values of β ^{23,24}. The comparison of the expected LQ sensitivity at the upgraded HERA and at the TeVatron Run II is illustrated in Fig. 6 in the (β, M_{LQ}) plane, which shows the competitiveness and complementarity of both facilities.

It is also interesting to note that most recent measurements on atomic parity violation seem to indicate a $\sim 2\sigma$ discrepancy with the SM predictions, which could be accounted for by LQ exchange. A global fit of data from HERA, LEP, TeVatron and low-energy experiments was performed²⁶, showing domains in the (λ, M_{LQ}) plane which could describe all the datasets.

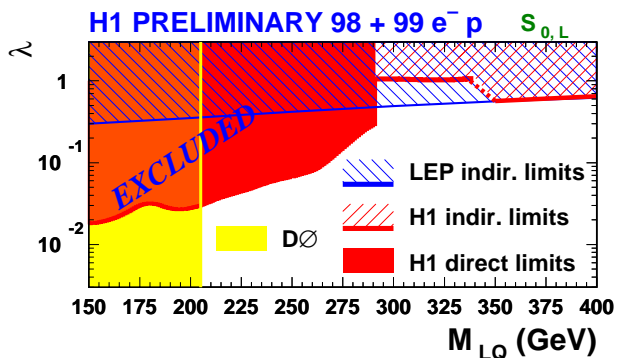


Figure 5: Mass-dependent upper bounds on the coupling λ for a $F = 2$ LQ decaying into eq and νq with an equal branching ratio of 50 %. Shaded (hashed) domains are excluded by direct (indirect) searches carried out at HERA, LEP and TeVatron.

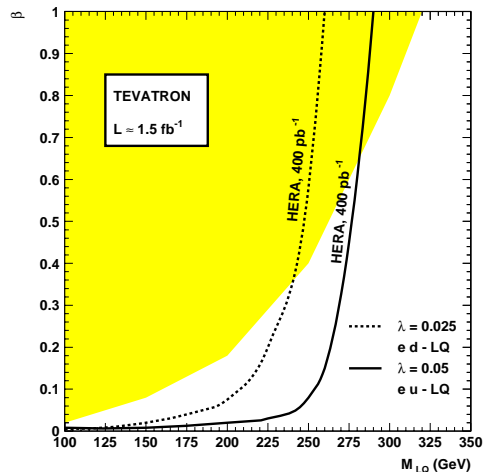


Figure 6: Expected mass-dependent sensitivities on the branching ratio β of a LQ decaying into eq at the upgraded HERA and at TeVatron II, indicated as full lines and shadowed domain respectively. Two typical cases are chosen for HERA's sensitivity.

8 Lepton Flavor Violation

From the neutrino experiments, it is likely that Lepton Flavor Violation (LFV) has been observed in the neutrino sector. It is thus crucial to look for LFV in the charged lepton sector as well. A possible source of LFV at HERA could be the exchange of LQ bosons that couple both to $e - q$ and to $\mu - q$ ($\tau - q$) pairs, denoted by λ_e and λ_μ (λ_τ) respectively, which would lead to $\mu + \text{jet}$ ($\tau + \text{jet}$) final states. Such final states have been looked for by both H1²³ and ZEUS²⁷, finding no events compatible with the kinematics of LQ-induced $eq \rightarrow lq$ processes. Upper bounds on the product $\lambda_e \times \sqrt{\beta_l}$, where β_l denotes the branching $\beta(LQ \rightarrow l + q)$, have thus been derived as a function of the LQ mass. These searches complement the hunting for 2nd and 3rd generation LQs carried out at the TeVatron²⁵, for which new results from an improved tagging of heavy flavors were reported.

The case of very high mass ($M_{LQ} \gg \sqrt{s}$) LFV LQs was also addressed by H1 and ZEUS. For both $e \leftrightarrow \mu$ and $e \leftrightarrow \tau$ transitions, direct constraints on such LQs obtained by HERA were compared to the most stringent indirect bounds. For some LQ types and $eq_i \leftrightarrow \tau q_k$ reactions, the HERA limits extend significantly beyond the reach of other experiments²⁷. Moreover, the luminosity upgrade will allow HERA to probe most of these transitions in a domain which is not covered by low-energy experiments, as shown in Fig. 7.

On the other hand, $e \leftrightarrow \mu$ transitions are much more constrained, by processes such as $\mu \rightarrow e\gamma$, $\mu \rightarrow 3e$, and $\mu - e$ conversion on heavy nuclei³⁸, whose

rates are experimentally constrained to be below $\sim 10^{-11} - 6 \times 10^{13}$. Even more stringent bounds are expected in the near future, which could shed light on the underlying non-SM physics responsible for LFV. It is important to note that, in non-supersymmetric models with massive neutrinos, the amplitudes of these processes are proportional to the neutrino square mass difference and thus extremely suppressed. However, in supersymmetric models they are only suppressed by inverse powers of the supersymmetry breaking scale, and (depending on the masses and mixings of superparticles) can lead to rates that are very close to the current bounds given above. Even for universality at M_{GUT} , renormalisation effects due to massive neutrinos will generate off-diagonal sfermion masses. What is actually very interesting is the correlation between the LFV processes in different supersymmetric theories. In the MSSM, $\mu \rightarrow e\gamma$, $\mu \rightarrow 3e$ and $\mu - e$ conversion all occur via one-loop diagrams, leading to approximate relations, e.g. $\Gamma(\mu^+ \rightarrow e^+e^+e^-)/\Gamma(\mu^+ \rightarrow e^+\gamma) \approx 6 \times 10^{-3}$. On the other hand, in the presence of R-parity violation, $\mu \rightarrow 3e$ and $\mu - e$ conversion may occur at tree-level. If, for instance, only $\lambda_{131}^*\lambda_{231}$ is non-zero, one finds that²⁸ $\Gamma(\mu \rightarrow e\gamma)/\Gamma(\mu \rightarrow 3e) = 1 \times 10^{-4}$ for $m_{\tilde{\nu}_3} = m_{\tilde{e}_R} = 100$ GeV, a very different prediction from the one in the MSSM with right-handed neutrinos.

9 Supersymmetry searches

The recent neutrino data seem to strongly indicate the presence of non-zero neutrino masses, and thus the existence of *beyond the Standard Model physics*. Among the various possibilities, supersymmetric theories are the most promising, since they also provide a solution to the hierarchy problem and consistent gauge unification. In this framework, the simplest model to search for is the so-called Minimal Supersymmetric Standard Model (MSSM), where sparticles are only produced in pairs and the lightest supersymmetric particle (LSP) is stable and neutral, leading to missing energy signatures.

The limits for selectrons and smuons obtained at LEP2²⁹ are $m_{\tilde{e}} > 92$ GeV and $m_{\tilde{\mu}} > 85$ GeV respectively. For stau pair production, there exists a small excess in all four experiments. LEP2 also gives bounds for charginos and neutralinos: $m_{\chi^0} > 37.5$ GeV and $m_{\chi^\pm} > 101$ GeV. Finally, searches for squark and gluon pair productions at the TeVatron³⁰ give $m_{\tilde{q}} \geq 240$ GeV and $m_{\tilde{g}} \geq 230$ GeV, while for stop-squarks the bound drops to 130 GeV due to mixing effects. These limits will improve during the future TeVatron runs, while the mass reach will significantly increase at the LHC³¹.

Supposing that a signal is found, a fundamental question is how to deduce the supersymmetric parameters, in a way as model independent as possible. This can be done by the combined study of the total cross-sections and spin

correlation measurements, and an optimal channel is chargino pair production in e^+e^- collisions³².

So far, we have been focusing on the minimal supergravity scenario. However, one can search for alternative theories, such as those with gauge-mediated³³ (GMSB) or anomaly-mediated³⁴ (AMSB) supersymmetry breaking. Unlike supergravity, where symmetry breaking occurs at M_{Planck} and is communicated via gravitational interactions to the observable sector, in gauge mediation this breaking occurs at a scale $\sqrt{F} \approx 100$ TeV and is communicated via gauge interactions and a so-called “messenger-sector”. The generic signatures are the existence of a super-light gravitino \tilde{G} and processes such as $\chi \rightarrow \gamma\tilde{G}$ or $\tilde{\ell}^\pm \rightarrow \ell^\pm\tilde{G}$. So far, no signal has been detected at LEP2 or TeVatron, leading to the bounds $\sqrt{F} > 217$ GeV and $m_{\tilde{G}} > 1.1 \times 10^{-5}$ eV. Moreover, LEP searches³⁵ for pair-produced \tilde{e} where $\tilde{e} \rightarrow \chi_1^0 \rightarrow \gamma\tilde{G}$ allow to almost rule out the interpretation of the CDF $ee\gamma\gamma E_{miss}$ event in GMSB models with a \tilde{G} LSP, as shown in Fig. 8.

In AMSB^{34,36} theories, supersymmetry breaking is originated by a rescaling anomaly and the superparticle spectrum is expressed in terms of beta-functions. A generic prediction is $M_1 > M_2$, leading to very light charginos and therefore a characteristic associated phenomenology³⁷.

Until now, we discussed the status of searches for supersymmetry with the minimal Yukawa sector. In the most general case, we can also have contributions violating lepton or baryon number, in combinations such that the proton is still stable (R -parity (R_p) violating supersymmetry). The new operators have the form $L_i L_j \bar{E}_k$, $L_i Q_j \bar{D}_k$ and $\bar{U}_i \bar{D}_j \bar{D}_k$ where L (Q) are the superfields containing the left-handed leptons (quarks) doublets, \bar{E} (\bar{D} , \bar{U}) those describing the right-handed singlets, and i, j, k are generation indices. In general, searches for SUSY with R_p violation at LEP²⁹ and TeVatron³⁰ provide a sensitivity on sparticle masses which is similar to that obtained with R_p conservation. For HERA, an optimal search channel for R_p -violating supersymmetry is through resonant single squark production via an $L_1 Q \bar{D}$ operator²⁴. This process is similar to single scalar leptoquark production, however in R_p violation we also have to consider the cascade decays of squarks to neutralinos and charginos. Especially for $L_1 Q_{2,3} \bar{D}_1$, one finds that the HERA limits can be better than those from alternative processes, such as atomic parity violation, for squark masses below 210 GeV. Finally, in the case that two R_p -violating operators involving different lepton flavours are large, HERA gives strong bounds on products of $(L_1 Q \bar{D})(L_3 Q \bar{D})$ operators, in analogy with the results for scalar leptoquarks²⁷ reported in section 8.

10 Higgs searches

In the SM a Higgs particle, H , is predicted by the spontaneous breaking of the electroweak symmetry, while the minimal supersymmetric extension of the theory requires two Higgs doublets, leading to two neutral CP-even states (h, H), one neutral CP-odd (A) and two charged ones (H^\pm). At tree-level, the mass of the lightest scalar Higgs boson h is restricted to be $m_h < M_Z$, however, radiative corrections drive this bound to $m_h \leq 135$ GeV. Thus, it is a generic prediction that supersymmetry leads to a light Higgs.

The direct SM Higgs search at LEP2 leads to a lower bound⁵ of 108 GeV. At the upgraded TeVatron experiment, the SM Higgs can be mainly produced via gluon fusion $gg \rightarrow H$ and the Drell–Yan like production $q\bar{q} \rightarrow W^* \rightarrow WH$. However, due to QCD backgrounds, the best channel is the Drell–Yan like process^{39,40}. Higgs discovery may also be possible via the $H \rightarrow \tau^+\tau^-$ decay in $H + W/Z$, while $gg \rightarrow H \rightarrow W^*W^* \rightarrow \ell\nu jj, \ell^+\ell^-\nu\bar{\nu}$ is also distinguishable owing to strong angular correlations among the final state leptons. A discovery of the SM Higgs boson at the upgraded TeVatron with $\mathcal{L} \approx 30 \text{ fb}^{-1}$ might be possible for $m_H \leq 125$ GeV and for $155 \leq m_H \leq 175$ GeV, while for $\mathcal{L} \approx 10 \text{ fb}^{-1}$ a 95% confidence level limit for $m_H < 180$ GeV can be provided. Finally, at the LHC, an important channel (not good for TeVatron) will be $gg \rightarrow H \rightarrow ZZ^* \rightarrow 4\ell^\pm$.

In the case of supersymmetry, the light scalar Higgs boson h can be mainly produced via $q\bar{q} \rightarrow W/Z + h$ analogously to the SM case. However, for large $\tan\beta$, the channels $q\bar{q}, gg \rightarrow b\bar{b} + h/A$ become important due to the large b -Yukawa couplings⁴⁰. A search for $b\bar{b}\Phi$ ($\Phi = h, H, A$) followed by $\Phi \rightarrow b\bar{b}$ has been performed by CDF and the results were converted into constraints in the plane ($\tan\beta, m_h$) which already cover a region which is not accessible at LEP, as shown⁴¹ in Fig. 9. In Run II the TeVatron will beautifully complement LEP by filling in a much larger part this region not covered by LEP.

Charged Higgs boson can also be searched for^{39,40}, while the effects of radiative corrections turn out to be significant and up to 100% in certain cases⁴⁰.

Finally, there also exists the possibility that no light scalar Higgs field exists, and symmetry breaking occurs due to the non-zero vacuum expectation values of composite operators, in the presence of strongly interacting gauge bosons at higher energies⁴². So far, the only probe for such theories comes from electroweak precision data. However one may hope to probe at the LHC or the linear collider anomalous four-boson effective vertices, which will be a strong indication for this type of physics.

11 Conclusions

In this workshop, the status of physics at highest Q^2 and p_t^2 was reviewed. Up to this extreme phase space, where all experiments face the limit of statistics, the SM predictions seem to beautifully describe the cross-sections over several orders of magnitude. These tests rather provide valuable information which constrains the parton-density functions of the proton and the photon. In the near-future programs of the HERA upgrade and the TeVatron Run II, substantial increase of statistics will help to further extend the available phase space, while in some measurements the developments in the precise theoretical calculation are becoming a crucial path for reducing errors.

Searches for hints of new physics are extensively carried out at HERA, LEP2 and TeVatron, and so far no definite signal has been observed. The complementarity of the colliders has been demonstrated in various searches, and some new possibilities were discussed. There are several 2σ -level “anomalies” seen, to be confirmed or disconfirmed with more data to come.

The DIS physics (which includes in a wider sense both lepton-parton and parton-parton scattering at short distance) will still play a major role in the next decade of particle physics. The ongoing physics study on how to search for Higgs and SUSY particles at the LHC is closely related to the outcome of the HERA and TeVatron runs in next few years, and these will definitely be an important topic at the “DIS 2010” workshop.

References

1. J. Repond, these proceedings.
2. F. Keil, these proceedings.
3. C. Royon, these proceedings.
4. B. Pöetler, these proceedings.
5. F. Terranova, these proceedings.
6. F. Machefert, these proceedings.
7. E. Rizvi, these proceedings.
8. A. Kappes, these proceedings.
9. H. Spiesberger, these proceedings.
10. K. Long, these proceedings.
11. J. Stirling, these proceedings.
12. P. Nason, R. Rückl and M. Spira, *J. Phys. G* **25**, 1434 (1999); M. Spira, in “Workshop on Monte Carlo Generators for HERA Physics” (DESY, 1998/99) 623.
13. U. Bassler, these proceedings.
14. N. Malden, these proceedings.

15. F. Olness, these proceedings.
16. S. Paganis, these proceedings.
17. A.S. Belyaev, these proceedings.
18. G Alemanni, these proceedings.
19. K. Hagiwara, S. Komamiya and D. Zeppenfeld, *Z. Phys. C* **29**, 115 (1985).
20. M.C. Cousinou, these proceedings.
21. I. Bertram, these proceedings.
22. H1 Collab., DESY-00-027; ZEUS Collab., *Eur. Phys. J. C* **14**, 239 (2000); also J. Scheins, these proceedings.
23. H1 Collab., *Eur.Phys.J. C* **11** (1999) 447.; ZEUS Collab., DESY-00-023.
24. A. Fox-Murphy, these proceedings.
25. D. Acosta, these proceedings.
26. A.F. Zarnecki, these proceedings.
27. R. Kerger, these proceedings.
28. K. Tobe, these proceedings.
29. S. Braibant, these proceedings.
30. N. Parua, these proceedings.
31. A. Parker, these proceedings.
32. J. Kalinowski, these proceedings.
33. See the review by G. Giudice and R. Rattazzi, *Phys. Rept.* **322** (1999) 419 and references therein.
34. L. Randall and R. Sundrum, *Nucl. Phys. B* **557** (1999) 79.
35. L3 Collab., L3 Note 2523, submitted to 2000 winter conferences.
36. B. Allanach, these proceedings.
37. J.L. Feng and T. Moroi, *Phys. Rev. D* **61** (2000) 095004.
38. Y. Kuno and Y. Okada, hep-ph/9909265 and references therein.
39. P. Ratoff, these proceedings.
40. M. Spira, these proceedings; M. Spira, hep-ph/9810289.
41. P. Janot, "Priorities for LEP in 2000", <http://alephwww.cern.ch/janot>
42. DIS2000 talk by J. Forshaw, "Mini review of physics without a light Higgs".

$q_i q_j$	$S_{1/2}^L$	$S_{1/2}^R$	$\tilde{S}_{1/2}^L$	V_0^R	V_0^L	\tilde{V}_0^R	V_1^L
1 1							
1 2							
1 3	-					-	
2 1							
2 2							
2 3	-					-	
3 1	-					-	
3 2	-					-	
3 3	-					-	

Figure 7: Future HERA's potential ($\mathcal{L} \sim 1 \text{ fb}^{-1}$) for LFV LQs coupling to $e - q_i$ and $\tau - q_j$. The columns correspond to LQs carrying different quantum numbers. Dark grey slots indicate cases where HERA will set the most stringent bound. For light grey slots, this should be the case provided that limits from rare B decays do not improve by more than a factor of two.

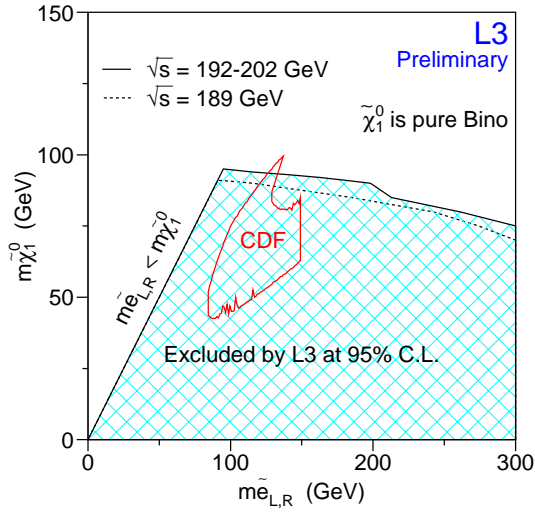


Figure 8: Domain excluded by L3 from searches for pair-produced selectrons where $\tilde{e} \rightarrow \chi_1^0 \rightarrow \gamma \tilde{G}$, in the plane spanned by the masses of the lightest neutralino χ_1^0 and of the selectron. The region of this plane where GMSB models with a \tilde{G} LSP could account for the $ee\gamma\gamma E_{miss}$ event observed by CDF is also represented.

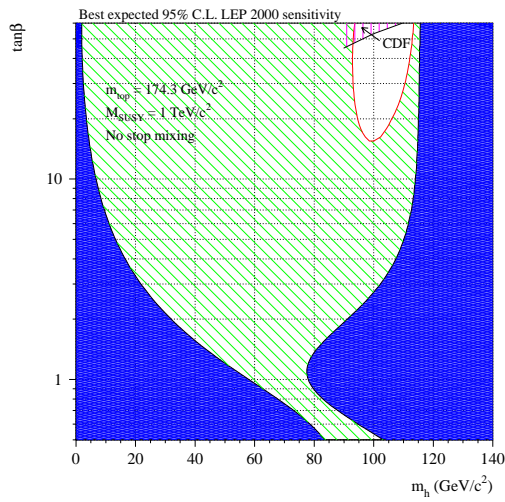


Figure 9: Projected LEP2 contours of the 95 % CL exclusion limits for MSSM Higgs sector parameters, as a function of $\tan\beta$ and m_h . The contours shown assume no stop mixing, leading to the maximal expected LEP coverage. The dark shaded region is theoretically forbidden. The domain currently excluded by CDF is also represented.